APPROXIMATE ACTUATOR DISK MODEL OF A ROTOR DURING HOVER OR AXIAL FLIGHT

Aviv Rosen
Faculty of Aerospace Engineering
Technion - Israel Institute of Technology
Haifa 32000, Israel.

Abstract

During recent years it became clear that wake distortion effects of rotors that pitch or roll, play a very important roll in helicopters' flight mechanics, especially their off-axis response. Almost all the models of wake distortion that have been reported in the literature, are vortex models. Yet, most of the models that are used in flight mechanics simulations are dynamic-inflow models, or the more sophisticated Finite State models. These are not vortex models, and thus in order to extend them to include wake distortion effects, additional assumptions have been adopted. Moreover, there are fairly large differences between the various models that were presented. In the present paper a new actuator disk model is presented that leads to a system of equations that are similar to the classical dynamic-inflow equations when disk rates are neglected. On the other hand these equations include wake distortion effects that are obtained through a unified consistent derivation. The model is obtained by applying two different approaches: Use of the incompressible and inviscid aerodynamic momentum equations and a vortex model. These two approaches, under certain assumptions, lead to identical forms of the equations. The model is approximate in the sense that it is based on certain simplifying assumptions. The new model gives an interesting insight into wake distortion effects. The results of the derivation are studied and compared with previous results from the literature.

1. Introduction

The "mystery" of the off-axis response[1], namely the incapability (up until recently) of helicopter simulation models to predict correctly the direction of the off-axis (cross-coupling) response to pilot cyclic stick command, was the center of many investigations during the last decade. It was first pointed out by Rosen and Isser[2] that the wake distortion (denoted geometric effects in that paper) due to the disk pitch or roll motion, has a significant influence on the induced velocities and results in a change in the direction of the off-axis response. The same authors showed[3] that these effects also result in the low damping in pitch and roll of rigid rotors. The model of Refs. 2,3 is a prescribed wake model that takes into account unsteady aerodynamic effects, thus it is capable of considering frequency influences on the effect. This unsteady predescribed wake model is fairly complicated and requires a significant computational effort that makes this model impractical for typical flight mechanics simulations.

Aerodynamic models that are suitable for flight mechanics purposes are actuator-disk models. The most popular among these models is probably the dynamic-inflow model of Pitt and Peters[4]. This model describes a three state unsteady rotor inflow distribution that is governed by the rotor thrust, as well as the aerodynamic pitch and roll moments. This model was later on extended to the Finite State Unsteady Wake Model[5], that includes higher harmonic functions for azimuthal load distribution (as compared to the three functions of the dynamic-inflow model), as well as a higher number of radial shape functions described by Legendre polynomials. Originally the dynamic-inflow model did not include the effect of wake distortion. Keller[6] was the first to introduce this effect into the dynamic-inflow formulation. It was done by introducing the wake distortion parameter due to angular rate, K_R, into the regular three ordinary differential equations of the dynamic inflow approach. The value of K_R was calculated based on modeling the wake of a hovering rotor as a vortex tube, namely replacing the actual rotor with an infinite number of blades with constant bound circulation, while neglecting wake contraction. The straight vortex tube in hover, is replaced by a curved vortex tube that is associated with a steady pitch or roll rates. K_R was calculated to be 1.5. In Ref. 7 system identification methods were applied to determine the wake distortion parameters, which are required to match between the off-axis response of both linear and nonlinear models, and flight test results. The authors obtained values of $K_R \approx 3$ that are twice the theoretical value of 1.5 (both are for hover).

References 6 and 7 were followed by other publications where the value of K_R was calculated using different vortex models. Krothapalli, Prasad, Peters and Barocela[8-11] presented a series of investigations. In Ref. 8 the momentum theory was used to obtain the value of K_R for hover and forward flight, and then combined it with an actuator disk theory. They obtained a value of $K_R = 0.5$ for hover and $K_R = 1$ for vertical climb, compared to the hover value of $K_R = 1.5$ of Ref. 7. In Ref. 9 a vortex lattice model was used. For axial flight a value

of $K_R = 1$ was obtained that agrees with the results of the momentum theory. In hover a value of $K_R = 0.5$ was obtained that again agrees with the momentum theory, but in addition an effective doubling of the wake curvature was observed, that offsets the reduction of K_R. In Ref. 10 a model for wake distortion in hover was augmented using results of a vortex tube representation. For hover a value of $K_R = 1.0$ was obtained and the authors indicated that the difference from Keller's model ($K_R = 1.5$) was due to the constant wake curvature assumption in Keller's approach. In Ref. 10 the authors also indicated that after using the vortex lattice method of Ref. 9 for 3, 4 and 5 bladed rotors, the average value for K_R effective was found to be approximately 1.33. This value was determined by calculating the effective moment on the rotor blade, rather than calculating the coefficient of the radial inflow distribution. In Ref. 11 the authors continued to emphasize the important influence of the contraction of the wake (in hover) on the effective curvature of the distorted wake. They used a value of $K_R = 1.33$, combined it with a generalized wake model, and obtained results that showed good agreement with wind tunnel flapping results of the SBMR rotor.

Free wake analysis is a natural candidate for an analysis where the wake distortion is important. Bagai, Leishman and Park[12,13] studied the aerodynamics of a rotor undergoing steady-state pitch or roll, using a free-vortex model of the wake. They obtained a value of $K_R \approx 2$ for hover, while the results were somewhat dependent on the pitch rate and blade lift distribution caused by blade twist. Another free wake model that approximates the wake as a series of vortex rings, was used by Basset and Tchen-Fo[14]. They showed the influence of vertical speed and rotor thrust on the value of K_R. For hover a value of $K_R = 1.6$ was obtained that agrees with the value obtained in Ref. 6.

Keller and Curtiss[15] extended their initial studies, using a prescribed (rigid) wake approach to study the influence of advance ratio on wake distortion effects, during steady pitch or roll. They also applied their model to investigate the damping in pitch or roll of a hovering rigid rotor (the case that was investigated in Ref. 3). They found that a value of $K_R = 1.1$ gave the best correlation with previously published test results, a value lower than the $K_R = 1.5$ that was obtained in their previous analyses.

Various investigators implemented the dynamic-inflow model, extended to include the wake distortion effect, into simulation codes, and identified the values of K_R that gave the best correlation with flight test results. Hamers and Grunhagen[16] concluded that good results for a BO-105 in hover are obtained if $K_R = 1.5$. He Chengjian, Lee and Chen Weibin[17] used $K_R = 1.20$ for a typical rotor thrust coefficient of 0.07. The inclusion of the wake distortion effect in a finite state dynamic wake model resulted in the correct trend of the pitch/roll off-axis response, but still underestimating the magnitude of the off-axis response. Including unsteady airloads provided very minor further improvement (this conclusion was in agreement with the results of Ref. 13), thus indicating that the intensity of the wake distortion effect is probably underestimated. Theodore and Celi[18] presented comparisons between the results of simulations using various values of $K_R (1, 1.5, 2)$, and also comparing the results with a free wake analysis. It was shown that different values of K_R give better agreement with the flight test results at different stages of the maneuver. The free wake model predicted the off-axis response more accurately than the extended dynamic-inflow model. In Ref. 19 the wake distortion was taken into account using a K_R coefficient within the Pitt and Peters dynamic inflow model. In the investigated case of an isolated articulated rotor[19], using a regular value of K_R from the literature, the effect of wake distortion was found to be small and the amount of coupling was underestimated compared to what would be needed to improve the correlation between the calculations and wind tunnel results. The results of Ref. 19 were in contrast to previous comparisons with flight test results, as well as new results that were presented in Ref. 20. Hamers and Basset[20] presented comparisons between results of simulations and flight test results of a BO-105 and a Dauphin performing a Dutch-roll. In the simulations they used Pitt and Peters dynamic-inflow model and the more complicated Finite State Unsteady Wake model of Ref. 5. For both models the wake distortion factor at hover was set to $K_R = 1.5$ showing good agreement with flight test results.

The above survey was confined to hover or axial flight since this is the subject matter of the present paper. Yet it is worth pointing out that few of the references included also forward flight analyses.

Based on the above literature survey the following conclusions are drawn:

a) The wake distortion effect due to rotor pitch and roll is strong at hover and diminishes with increasing velocity. It is essential to take this effect into account in order to obtain satisfactory agreement with the off-axis response measured in flight tests or wind-tunnel experiments. This effect usually does not result in a deterioration of the on-axis results, and in many cases it even improves them in comparison with measurements.

b) Dynamic-inflow models, or the more detailed Finite State Unsteady Wake models, are commonly used for flight mechanics simulations and other purposes. These models can be

extended to take into account wake distortion effects, by introducing the wake distortion coefficient K_R. This coefficient is influenced by the magnitude of the axial velocity.

c) Almost all previous calculations of the wake distortion coefficients were based on a vortex modeling of the wake. There are very significant variations between the values of the coefficients that have been reported in the literature. The calculated values for hover range between $K_R = 0.5$ and $K_R > 2$.

d) Various studies in the past indicated that the values of K_R that were obtained by various theoretical derivations, underestimate the intensity of the effect. In certain hover cases values of $K_R \approx 3$ were found to give the best agreement with flight test results.

e) The first detailed model of the wake distortion[2,21] included the effect of pitch and roll rate variations. Yet all the models that were developed to calculate the wake distortion coefficients, assumed steady pitch or roll. The importance of modeling the transient behavior of the rotor wake was pointed out by Curtiss[22], but he did not present a model that deals with the issue.

The purpose of the present paper is to present a new approximate actuator-disk model for hover and axial flight, that will address few of the problems that were pointed out above (based on the literature survey). Unlike previous derivations where the wake distortion coefficients were calculated using a vortex wake model and then added to a dynamic-inflow model that was obtained using a different approach, the derivation of the wake distortion effects in the present paper will be an integral part of the derivation of the entire model.

The present model will be derived using two different approaches:

a) Using the momentum equations of an inviscid, incompressible fluid.

b) A vortex model.

The new model will not be confined to constant pitch or roll rates, but it will also consider time variations of the angular rates. The results of the two approaches will be compared and conclusions drawn. Results of the model will also be compared with experimental results from the literature.

2. Derivations Based on Using the Momentum Equations of an Inviscid and Incompressible Fluid

2.1 General Derivation

Two systems of coordinates are used: a Cartesian system (x ,y, z) and a cylindrical system (r, ψ, z). The origin and z axis of both systems coincide. x, y, z and r are non-dimensional and obtained after dividing the dimensional coordinates by the disk radius, R.

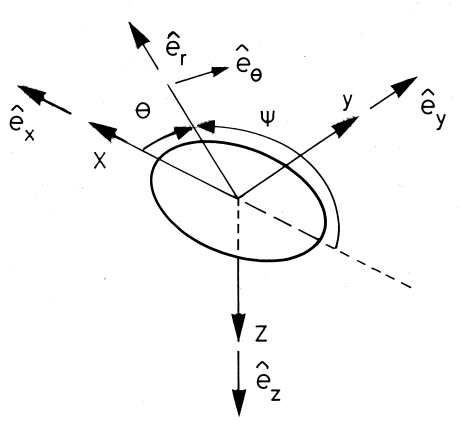

Fig. 1: The Cartesian and cylindrical systems of coordinates.

Small perturbations about a basic state of hover or axial flight are considered. The basic state is axisymmetric, and thus described by the non-dimensional axial and radial components of the flow relative to the disk, V_z and V_r, respectively. Equations for flow in a cylindrical system of coordinates can be found in Ref. 23.

The perturbations about the basic state include a non-dimensional axial velocity of the disk, u_D, and the non-dimensional pitch and roll rates of the disk, q_D and p_D, about the axes y and x, respectively. The non-dimensional angular rates are obtained after dividing the dimensional angular rates by the rotor angular speed, Ω.

The systems of coordinates are attached to the disk: The origin coincides with the disk center, the coordinates x, y, r lie in the disk plane and z perpendicular to it. The non-dimensional perturbation in the axial velocity of the flow, relative to the disk coordinates system, is u_z. The non-dimensional perturbation in the pressure (about the basic state) is s (the dimensional pressure is divided by $\rho_A \Omega^2 R^2$, where ρ_A is the air mass density). The equation for u_z becomes (see Ref. 31):

$$\overset{*}{u}_z + V_r \frac{\partial u_z}{\partial r} + \underline{\frac{\partial V_z}{\partial r} u_r} + V_z \frac{\partial u_z}{\partial z} + \frac{\partial V_z}{\partial z} u_z + \overset{*}{u}_D + r(\overset{*}{q}_D \cos\psi + \overset{*}{p}_D \sin\psi) + 2V_r(q_D \cos\psi + p_D \sin\psi) = -\frac{\partial s}{\partial z} \qquad (2.1)$$

$(^*)$ indicates differentiation with respect to a non-dimensional time, Ωt.

The present derivation will be confined to cases where the axial velocity in the basic state is uniform over each cross-section of the flow (namely, a plane z = const). Thus the underlined term in the last equation can be neglected.

In what follows perturbations about two basic states will be considered: a rotor in a fast axial flight and a rotor in hover.

2.2 A Rotor in a Fast Axial Flow

In this case:

$$V_r \cong 0 \quad ; \quad V_z = V_c \tag{2.2}$$

where V_c is the velocity of the axial incoming flow in the basic state.

Substitution of Eq. (2.2) into Eq. (2.1) results in the following equation:

$$\overset{*}{u}_z + V_c \frac{\partial u_z}{\partial z} + \overset{*}{u}_D + r(\overset{*}{q}_D \cos\psi + \overset{*}{p}_D \sin\psi) = -\frac{\partial s}{\partial z} \tag{2.3}$$

Similar to the classical dynamic-inflow approach, taking only the first three harmonics from a more general solution, it is assumed that:

$$u_z = w_{zo} f_0(z) + (w_{zs} r \sin\psi + w_{zc} r \cos\psi) f_1(z) - u_D - r(p_D \sin\psi + q_D \cos\psi) \tag{2.4}$$

w_{zo}, w_{zs} and w_{zc}, as well as u_D, q_D and p_D, are functions of time.

The functions $f_0(z)$ and $f_1(z)$ satisfy the following conditions:

$$f_0(0) = f_1(0) = 1 \; ; \; f_0(-\infty) = f_1(-\infty) = 0 \; ; \quad f_0(\infty) = a_0 \; ; \; f_1(\infty) = a_1 \tag{2.5}$$

a_0 and a_1 represent the increase in the induced velocity far behind the rotor. According to the momentum theory a_0 and a_1 are equal to 2. Yet is should be noted that various sources, as early as Ref. 24, indicate that a_0 and probably a_1 may differ from 2.

It is clear that Eq. (2.4) satisfy the conditions at $z = -\infty$. The functions $f_0(z)$ and $f_1(z)$ will change as a result of an increase in the rate of change with time. The present derivation will concentrate on harmonic perturbations, having a frequency ω. Thus $f_0(z)$ and $f_1(z)$ are in general functions of the frequency ratio k (k = ω/Ω).

The non-dimensional pressure is chosen to also include the first three harmonics:

$$s = -s_0 f_0(z)/a_0 + (s_s r \sin\psi + s_c r \cos\psi) f_1(z)/a_1 \quad \underline{\text{for}} \quad z < 0 \tag{2.6a}$$

$$s = -s_0 [f_0(z)/a_0 - 1] + (s_s r \sin\psi + s_c r \cos\psi)[f_1(z)/a_1 - 1] \quad \underline{\text{for}} \quad z > 0 \tag{2.6b}$$

s_0, s_s and s_c are in general functions of time.

The last equations satisfy the condition of zero pressure perturbations at $z = \pm\infty$. It allows a pressure jump across the disk, Δs, where:

$$\Delta s = s_0 - s_s r \sin\psi - s_c r \cos\psi \tag{2.7}$$

Simple integration over the disk indicates that:

$$s_0 = \Delta C_T \; ; \; s_s = 4\Delta C_{LA} \; ; \; s_c = 4\Delta C_{MA} \tag{2.8}$$

where ΔC_T, ΔC_{LA} and ΔC_{MA} are the perturbations in the disk aerodynamic: thrust coefficient, roll moment coefficient and pitch moment coefficient, respectively. They are in general functions of time.

Substitution of Eq. (2.4) into Eqs. (2.6a,b), using an approximation method to replace the functions of z by parameters that are in general functions of k (any weighting residuals method, like Galerkin method or collocation method, is a natural candidate for this approximation procedure, see Ref. 25) and comparing harmonics, lead to the following system of differential equations:

$$[M_c]\{\overset{*}{w}\} + [L_c]^{-1}\{w\} = \{\Delta C\} \tag{2.9}$$

where:

$$[M_c] = \begin{bmatrix} m_0(k) & 0 & 0 \\ 0 & m_1(k) & 0 \\ 0 & 0 & m_1(k) \end{bmatrix} \tag{2.10a}$$

$$[L_c]^{-1} = V_c \begin{bmatrix} a_0 & 0 & 0 \\ 0 & -a_1/4 & 0 \\ 0 & 0 & -a_1/4 \end{bmatrix} \tag{2.10b}$$

$$\{w\}^T = < w_{zo}, w_{zs}, w_{zc} > \tag{2.10c}$$

$$\{\Delta C\}^T = < \Delta C_T, \Delta C_{LA}, \Delta C_{MA} > \tag{2.10d}$$

Equation (2.9) has the same form as the dynamic inflow equation of Pitt and Peters[4]. Moreover, if the values of a_0 and a_1 according to the momentum theory are chosen equal to 2, the matrix $[L_c^{-1}]$ of Eq. (2.10b) is identical to the same matrix in Ref. 4. The matrix [M] has the same form as in Ref. 4, but the actual values of the diagonal elements depend on the approximation approach of replacing the functions of z.

The distribution of the axial component of the induced velocity through the disk, ν, is (see Eqs. (2.4), (2. 5)):

$$\nu = w_{zo} - u_D + r[(w_{zs} - p_D)\sin\psi + (w_{zc} - q_D)\cos\psi] \tag{2.11}$$

It should be noted that ν is given relative to the axially moving, pitching and rolling system of coordinates. In many cases and applications (most of the simulation codes for example) the induced velocity at the disk is described relative to an inertial system that coincides at each moment with the pitching and rolling system (either x, y, z or r, θ, z). The induced velocity in this case is denoted λ:

$$\lambda = \lambda_0 + r(\lambda_s \sin\psi + \lambda_c \cos\psi) \tag{2.12}$$

The relation between ν and λ is:

$$\lambda = \nu + u_D + r(p_D \sin\psi + q_D \cos\psi) \tag{2.13}$$

It turns out that according to Eqs. (2.11-13), for the case of a fast axial flight:

$$\lambda_0 = w_{zo} \; ; \; \lambda_s = w_{zs} \; ; \; \lambda_c = w_{zc} \tag{2.14}$$

Equation (2.14) indicates that in the case of a fast unsteady axial flight, the influence of wake distortion disappears if the induced velocity is measured relative to an inertial system.

2.3 A Rotor in Hover

In the case of hover the basic state includes only axially symmetric induced velocities. As indicated above, it is assumed that V_z is uniform over each cross-section of the wake, therefore:

$$V_z = V_{zo} g(z) \tag{2.15}$$

where:

$$g(0) = 1 \; ; \; g(-\infty) = 0 \; ; \; g(\infty) = b \tag{2.16}$$

V_{zo} is the nondimensional induced axial velocity through the disk, in the basic state. $V_{zo} b$ is the induced velocity far beneath the rotor, in the basic state. According to the momentum theory b = 2.

If Eq. (2.15) describes the basic axial induced velocity, a radial induced velocity that satisfies the continuity equation is:

$$V_r = -\frac{1}{2} V_{zo} r \, g'(z) \tag{2.17}$$

Substitution of Eqs. (2.15) and (2.17) into Eq. (2.1) results in the following equation for hover:

$$\overset{*}{u}_z - \frac{1}{2} V_{zo} r \, g'(z) \frac{\partial u_z}{\partial r} + V_{zo} g(z) \frac{\partial u_z}{\partial z} + V_{zo} g'(z) \, u_z + \overset{*}{u}_D + r \, (\overset{*}{q}_D \cos\psi + \overset{*}{p}_D \sin\psi) - V_{zo} r \, g'(z)(q_D \cos\psi + p_D \sin\psi) = -\frac{\partial s}{\partial z} \tag{2.18}$$

Interesting quasi-solutions of Eq. (2.18) can be obtained and are presented in Ref. 31, but they are not presented here because of lack of space. Based on these solutions it is assumed that:

$$u_z = w_{zo} f_o(z) - u_D + r(w_{zs} \sin\psi + w_{zc} \cos\psi) g(z) + r[w_p h(z) - p_D] \sin\psi + r[w_q h(z) - q_D] \cos\psi \tag{2.19}$$

$w_{zo}, w_{zs}, w_{zc}, w_p$ and w_q are functions of time. $f_o(z)$ and g(z) satisfy the conditions of Eqs. (2.5) and (2.16), respectively. h(z) is a continuous function of z, that satisfies the following conditions:

$$h(0) = 1 \tag{2.20a}$$

$$|h'(z)| << |g'(z)| \quad \underline{\text{for}} \quad -1 << z << 1 \tag{2.20b}$$

$$h(-\infty) = 0 \tag{2.20c}$$

It is well known that the wake contraction is fairly fast and occurs very close to the disk. Thus g'(z) obtains finite values near the disk, but it drops to very small values (practically zero) as the distance from the disk increases. Equation (2.20b) expresses the assumption that near the disk h(z) changes much slower than g(z).

It is clear, based on Eqs. (2.20a-c), that Eq. (2.19) satisfies the conditions at $z = -\infty$.

The nondimensional perturbation in the pressure, s, is chosen as:

$$s = -\Delta C_T \, g(z) f_0(z)/(a_0 b) + 4 r (\Delta C_{LA} \sin\psi + \Delta C_{MA} \cos\psi) g(z) f_1(z)/(a_1 b) \quad \underline{\text{for}} \quad z < 0 \tag{2.21a}$$

$$s = -\Delta C_T [g(z) f_0(z)/(a_0 b) - 1] + 4 r (\Delta C_{LA} \sin\psi + \Delta C_{MA} \cos\psi)[g(z) f_1(z)/(a_1 b) - 1] \quad \underline{\text{for}} \quad z > 0 \tag{2.21b}$$

Substitution of Eqs. (2.19) and (2.21a,b) into Eq. (2.18), using again an approximation method to replace the functions of z by parameters that are functions of k, and comparing harmonics, lead to the following set of differential equations:

$$m_1(k) \overset{*}{w}_{zo} + V_{zo} a_o b \, w_{zo} = \Delta C_T + V_{zo} m_2(k) u_D \tag{2.22a}$$

$$[M_H^1]\{\overset{*}{w}_m\} + [L_H^1]^{-1}\{w_m\} = \{\Delta C_m\} \tag{2.22b}$$

$$[M_H^2]\{\overset{*}{w}_r\} + [L_H^2]\{w_r\} = \{\omega\} \tag{2.22c}$$

The vectors and matrices that appear in Eqs. (2.22b,c) are defined below:

$$[M_H^1] = \begin{bmatrix} m_3(k) & 0 \\ 0 & m_3(k) \end{bmatrix} \tag{2.23a}$$

$$[L_H^1]^{-1} = V_{zo} \begin{bmatrix} -\frac{3b^2}{16} & 0 \\ 0 & -\frac{3b^2}{16} \end{bmatrix} \tag{2.23b}$$

$$[M_H^2] = \frac{1}{V_{zo}} \begin{bmatrix} m_4(k) & 0 \\ 0 & m_4(k) \end{bmatrix} \tag{2.23c}$$

$$[L_H^2] = \begin{bmatrix} m_5(k) & 0 \\ 0 & m_5(k) \end{bmatrix} \tag{2.23d}$$

$$\{w_m\}^T = < w_{zs}, w_{zc} > \tag{2.23e}$$

$$\{\Delta C_m\}^T = < \Delta C_{LA}, \Delta C_{MA} > \tag{2.23f}$$

$$\{w_r\}^T = < w_p, w_q > \tag{2.23g}$$

$$\{\omega\}^T = < p_D, q_D > \tag{2.23h}$$

The axial nondimensional induced velocity through the disk, ν, is (see Eq. (2.19)):

$$\nu = u_z(z=0) = w_{zo} - u_D + r[(w_{zs} + w_p - p_D)\sin\psi + (w_{zc} + w_q - q_D)\cos\psi] \tag{2.24}$$

$w_{zo}, w_{zs}, w_{zc}, w_p$ and w_q are obtained after solving Eqs. (2.22a-c).

The nondimensional axial induced velocity through the disk, relative to an inertial system of coordinates that coincides (at the moment of observation) with the moving pitching and rolling system, λ, is defined by Eqs. (2.12) and (2.13). Using these equations and Eq. (2.24), results in the following expressions:

$$\lambda_o = w_{zo} \quad ; \quad \lambda_s = w_{zs} + w_p \quad ; \quad \lambda_c = w_{zc} + w_q \tag{2.25}$$

w_{zo}, w_{zs} and w_{zc} are obtained by solving Eqs. (2.22a,b). w_p and w_q are obtained by solving Eq. (2.22c).

In most of the previous investigations, instead of using separate equations for the two pairs of

unknowns: (w_{zs}, w_{zc}) and (w_p, w_q), two equations were used for the sums: $(w_{zs} + w_p)$ and $(w_{zc} + w_q)$. This is convenient since (see Eq. 2.25) λ_s and λ_c, respectively, are obtained. From Eqs. (2.22b,c) it is clear that the replacement of the four equations by only two equations can be performed if:

$$[M_H^1] = \gamma [M_H^2] \quad (2.26a)$$

$$[L_H^1]^{-1} = \gamma [M_H^2] \quad (2.26b)$$

where γ in general may be a function of k.
In this case the equation for the induced velocity relative to an inertial reference system becomes:

$$[M_H^1]\{\overset{*}{\lambda}_m\} + [L_H^1]^{-1}\{\lambda_m\} = \{\Delta C_m\} + \gamma\{\omega\} \quad (2.27a)$$

$$\{\lambda_m\}^T = < \lambda_s, \lambda_c > \quad (2.27b)$$

It should be noted that the wake distortion effect in the present derivation is a direct result of taking into account the radial induced velocities in the basic state (Coriolis accelerations). In light of this it is interesting to note that Refs. 10, 11, based on a completely different approach and obtaining different results, pointed out the important influence that contraction may have on the distortion effect.

3. Derivations Based on a Vortex Model

As in the previous section, the derivations here are also concerned with small perturbations about a basic state of hover or axial flight. At first the basic state will be defined. Then perturbations about this basic state will be considered.

In order to obtain a disk theory, an infinite number of blades is assumed. This assumption has been used by many researchers in the past and is presented for example in Refs. 26-28. It was shown in Ref. 27 (page 166) that this assumption is equivalent to the time averaged induced velocity of a rotor having a finite number of blades.

In the present analysis the blades are presented as lifting lines. As a result of variations in the circulation along the blade, trailing vortices leave its trailing edge. Due to time variations of the bound circulation, shed vortices are also leaving the blade. The trailing and shed vortices form the wake.

The wake geometry has a major effect on the results. In the present analysis it will be assumed that each vortex element that leaves the blade cross-section moves axially with a velocity that is equal to the average axial velocity at that cross-section, in the basic state. This average axial velocity is the resultant of the incoming axial flow at infinity, and the average axial component of the induced velocity at that cross-section. The influences of the radial and tangential components of the induced velocity are neglected, as well as variations of the induced velocity along the wake.

In the present analysis harmonic perturbations are considered that have an identical frequency.

The systems of coordinates that will be used are attached to the disk center - moving, pitching and rolling with the disk. These are the same systems that were used in the previous section: A Cartesian system (x, y, z) and a cylindrical system [(r,ψ,z) or (ρ,μ,z)].

3.1 The Basic State

As in the previous section, the basic state includes an incoming nondimensional axial velocity V_c.

It is assumed that the wake in the basic state is comprised only of a tip vortex. The nondimensional axial velocity of each vortex element of this tip vortex, relative to the disk, is V_{tip}. In the case of a disk model (an infinite number of blades), the nondimensional axial velocity that is induced over the disk is uniform and equals (see Eq. (7.10) of Ref. 27)):

$$v_{io} = N_b \Gamma_{otip} / (4\pi V_{tip}) \quad (3.1)$$

Γ_{otip} is the nondimensional circulation of the tip vortex of each blade (in the basic state). Nondimensionalization of circulation is obtained after dividing the dimensional value by ΩR^2. N_b is the number of blades.

As indicated in Ref. 27 (p. 165), the nondimensional velocity that is induced at the blade tip, along the vortex cylinder, is $(v_{io}/2)$, therefore:

$$V_{tip} = V_c + v_{io}/2 \quad (3.2)$$

In the case of a fast axial flow:

$$V_{tip} \cong V_c \quad (3.3)$$

In the case of hover:

$$V_{tip} = v_{io}/2 \quad (3.4)$$

If Eq. (3.4) is substituted into Eq. (3.1), the following relation is obtained for hover:

$$N_b \Gamma_{otip} / \left(8\pi V_{tip}^2\right) = N_b \Gamma_c / \left(2\pi v_{io}^2\right) = 1 \quad (3.5)$$

The nondimensional axial velocity over the disk, relative to the disk plane, is denoted v_s:

$$V_s = V_c + v_{io} \quad (3.6)$$

It is clear that for a fast axial flow:

$$V_s \cong V_c \quad (3.7)$$

For hover:

$$V_s = v_{io} \quad (3.8)$$

3.2 The Perturbations about the Basic State

The perturbations about the basic state include three elements:

a) Perturbations in the disk position and orientation.
b) Perturbations in the aerodynamic loads along the blades.
c) Perturbations in the induced velocity over the disk.

The perturbations in the disk position and orientation at time τ, are defined by a

nondimensional axial motion, $\Delta z_D(\tau)$, and pitch and roll angles, $\Delta\theta_D(\tau)$ and $\Delta\phi_D(\tau)$, respectively, relative to the basic state. Since harmonic perturbations at a frequency ω are considered:

$$\Delta z_D(\tau) = \Delta z_D e^{i\omega\tau} \tag{3.9a}$$

$$\Delta\theta_D(\tau) = \Delta\theta_D e^{i\omega\tau} \tag{3.9b}$$

$$\Delta\phi_D(\tau) = \Delta\phi_D e^{i\omega\tau} \tag{3.9c}$$

$\Delta z_D, \Delta\theta_D$ and $\Delta\phi_D$ are complex amplitudes that represent magnitudes and phase shifts.

The perturbations in the aerodynamic loads that act on the blade are described as perturbations in the bound circulation. The circulation at the cross-section ρ of a blade at azimuth μ, at time τ, is:

$$\tilde{\Gamma}(\rho,\mu,\tau) = \Omega R^2[\Gamma_o(\rho) + (\Delta\Gamma_o + \Delta\Gamma_s\,\rho\sin\mu + \Delta\Gamma_c\,\rho\cos\mu)e^{i\omega\tau}] \tag{3.10}$$

$\Gamma_o(\rho)$ is the circulation in the basic state, while $\Delta\Gamma_o$, $\Delta\Gamma_s$ and $\Delta\Gamma_c$ are the perturbations.

The perturbation in the induced velocity is also harmonic with a frequency ω. Thus the nondimensional induced axial velocity over the disk, at time τ, relative to the disk, is:

$$v_i(r,\psi,\tau) = v_{io} + \Delta v_i(r,\psi)\cdot e^{i\omega\tau} \tag{3.11}$$

v_{io} is the induced velocity in the basic state.

$\Delta v_i(r,\psi)$ is the amplitude of the perturbation. The perturbation of the induced velocity is calculated using the Biot-Savart law. It is the sum of four contributions:

a) Perturbation in the circulation of the tip vortex.
b) Perturbations in the circulation of the trailing vortices of the inner field.
c) Shed vortices.
d) Wake distortion effects.

The detailed calculations are presented in Ref. 31.

Similar to the previous section, $\Delta v_i(r,\psi)$ is expressed as follows:

$$\Delta v_i(r,\psi) = \Delta v_{io} + \Delta v_{is}\,r\sin\psi + \Delta v_{ic}\,r\cos\psi + \Delta v_{ip}\,r\sin\psi + \Delta v_{iq}\,r\cos\psi \tag{3.12}$$

Δv_{is} and Δv_{ic} are dependent on the aerodynamic moments, while Δv_{ip} and Δv_{iq} depend on the angular rates and present wake distortion effects.

The complex equations for the five unknown coefficients are:

$$\Delta v_{io} = (J_{kco} + i\,k\,J_{kso}\,J_{tip2}\,J_v/V_s)\cdot\left(\frac{J_v\,\Delta C_T}{2\,d_{u0}V_s} + J_{wd}\,u_D\right) \tag{3.13a}$$

$$\begin{Bmatrix}\Delta v_{is}\\ \Delta v_{ic}\end{Bmatrix} = -\frac{1}{V_s d_{u1}}\begin{bmatrix}K_1 & K_2\\ -K_2 & K_1\end{bmatrix}\begin{Bmatrix}\Delta C_{LA}\\ \Delta C_{MA}\end{Bmatrix} \tag{3.13b}$$

$$\begin{Bmatrix}\Delta v_{ip}\\ \Delta v_{iq}\end{Bmatrix} = J_{wd}(J_{ks2} - i\,k\,J_{kc2}\,J_{tip2}\,J_v/V_s)\begin{Bmatrix}p_D\\ q_D\end{Bmatrix} \tag{3.13c}$$

$$K_1 = (J_v+1)\,J_{kc1} - i\,k\,J_{ks1}(J_{tip4}\,J_v + J_{ts2})/V_s \tag{3.13d}$$

$$K_2 = (k^2\,J_{ks1}\,J_{s2}/V_s + i\,k\,J_{kc1}\,J_{s1}) \tag{3.13e}$$

where:

$$J_v = V_s/V_{tip} \tag{3.14a}$$

$$J_{tip2} \cong 0.84 \tag{3.14b}$$

$$J_{tip4} \cong 0.17 \tag{3.14c}$$

$$J_{ts2} \cong 0.93 \tag{3.14d}$$

$$J_{s1} \cong 0.79 \tag{3.14e}$$

$$J_{s2} \cong 0.57 \tag{3.14f}$$

and:

$$J_{wd} = \frac{N_b\Gamma_{0\,tip}}{4\pi V_{tip}^2} \tag{3.15}$$

The coefficients $J_{tip2}, J_{tip4}, J_{ts2}, J_{s1}$ and J_{s2} represent linear approximations to more complicated functions of r.

d_{uo} and d_{u1} are complex numbers that represent unsteady aerodynamic characteristics of the cross-sectional lift force. In fact they are lift-deficiency coefficients of the cross-sections. In the present analysis these unsteady effects will be neglected, namely d_{uo} and d_{u1} will be taken equal to one.

$J_{kco}, J_{kc1}, J_{kc2}, J_{kso}, J_{ks1}$ and J_{ks2} are correction factors to approximations adopted during the derivations. These are approximations of sine and cosine functions, where only the first term in the series is included. All the corrections that will be used here have the form:

$$1/(1+c_1k^2/V_s^2)$$

This expression reminds of the next missing term in the series. The corrections start to be effective only at relatively high frequency ratios (high k values). These corrections can be found based on a more refined analysis. In what follows they will be chosen such that they will result in a good correlation with experimental or flight test results.

4. Comparison between the Two Models

According to Eqs. (3.3), (3.7), (3.14a) and (3.15), for a fast axial flow:

$$J_{wd} \cong 0 \quad ; \quad J_v = 1 \tag{4.1}$$

According to Eqs. (3.4), (3.5), (3.8), (3.14a) and (3.15), for hover:

$$J_v = 2 \quad ; \quad J_{wd} = 2 \tag{4.2}$$

In Ref. 31 a detailed comparison between the results of Sections 2 and 3 are presented. It is shown that full resemblance exists between the two and the

results of Section 3 can be used to obtain the matrices $[M_H^1]$, $[M_H^2]$ and $[L_H^2]$ of Eqs. (2.22a-c).

5. Results and Discussion

The model that was described above was implemented in a simulation code of a hovering helicopter. In this code the fuselage has six degrees of freedom that are described by three nondimensional velocity components of the center of mass (u_f, v_f, w_f - forward, to the right and downward, respectively) and the three nondimensional angular rates (p_f, q_f, n_f - roll, pitch and yaw rates, respectively). The hub center is located at a height h above the fuselage center of mass. The rotor degrees of freedom include rigid flapping and pitch angle variations. In the present analysis only the first three multiblade degrees of freedom are considered. The azimuth angle of blade n at time τ is $\psi(n,\tau)$. The flapping angle of that blade, $\beta(n,\tau)$, is:

$$\beta(n,\tau) = \beta_o(\tau) + \beta_c(\tau)\cdot\cos\psi(n,\tau) + \beta_s(\tau)\cdot\sin\psi(n,\tau) \tag{5.1}$$

The pitch angle of the same blade, $\theta(n,\tau)$, is:

$$\theta(n,\tau) = \theta_o(\tau) - A_1(\tau)\cdot\cos\psi(n,\tau) - B_1(\tau)\cdot\sin\psi(n,\tau) \tag{5.2}$$

Lead-lag motions of the blades are ignored.

The disk nondimensional axial velocity, u_D, roll rate, p_D, and pitch rate, q_D, are thus:

$$u_D = w_f - 0.75\cdot\overset{*}{\beta}_o(\tau) \tag{5.3a}$$

$$p_D = p_f - \overset{*}{\beta}_s(\tau) \tag{5.3b}$$

$$q_D = q_f - \overset{*}{\beta}_c(\tau) \tag{5.3c}$$

As indicated in section 2 above, an upper asterisk indicates differentiation with respect to the nondimensional time. The blade three-quarters spanwise cross-section is chosen as the representative point in Eq. (5.3a).

The complete model, as presented by Eqs. (3.13a-c), was implemented into the simulation code. Initial studies for different rotors at different basic states showed that the influence of the off-diagonal elements in Eq. (3.13b), the K_2 elements, is negligible. Therefore these elements will be neglected in what follows.

The correction coefficients will be:

$$J_{kc1} = 1 \tag{5.4a}$$

$$J_{ks1} = J_{kc2} = \frac{1}{1+k^2/V_{zo}^2} \tag{5.4b}$$

$$J_{ks2} = \frac{1}{1+0.5\,k^2/V_{zo}^2} \tag{5.4c}$$

In hover or axial flow the axial motion u_D and coning ($\beta_o(\tau)$) are usually only very slightly coupled with other degrees of freedom. Therefore the present study will concentrate on the more interesting pitch, roll and disk tilt degrees of freedom.

Two cases will be investigated:

a) The frequency response of a fixed shaft rotor in hover.
b) The frequency response of a hovering helicopter.

5.1 The Frequency Response of a Fixed Shaft Rotor in Hover

The flapping response of an articulated rotor in hover, to harmonic cyclic pitch variations, is investigated. The rotor is the one that was tested at the Modane S1 wind tunnel and results reported in Ref. 19. More details about the model and test procedure appear also in Refs. 29, 30.

The model has a radius of 2.1 m and a reference chord of 0.1593 m. The solidity is 0.0966 and the offset is 0.075 m. The aerodynamic characteristics are given in Ref. 19. Since a detailed data about the mass distribution was not available, typical characteristics have been assumed. This inaccuracy may result in certain inaccuracies in the results.

The on-axis flapping response, β_s/A_1, is presented in Fig. 2. Three kinds of calculations are shown:

a) A complete model.
b) A model that does not include wake distortion effects.
c) A complete model where the matrices $[M_H^1]$ and $[L_H^1]^{-1}$ in Eq. (2.22b) are replaced by the equivalent matrices of the dynamic inflow-model of Ref. 4.

Differences between the calculations appear only at relatively high frequencies. It is shown that the influence of wake distortion on the on-axis behavior is negligible. The changes in the aerodynamic matrices result in larger differences, increasing the differences between the experimental and calculated results.

There is a good agreement in the phase angle between the results of the complete model (with and without wake distortion) and the experimental results. In the case of the amplitude the experimental results are lower than the calculations and the difference seems to increase with the frequency. This difference appears also in Ref. 19. It probably indicates that a certain phenomenon is missing in the modeling of the rotor (mechanical damping, mechanical phase lag, etc.) that affects the quality of the results.

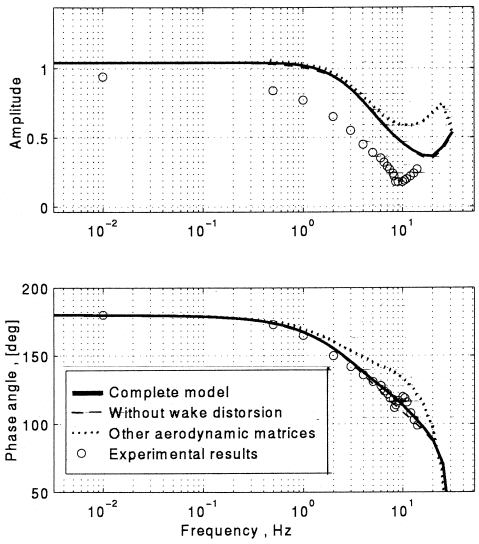

Fig. 2:The on-axis flapping response of a fixed shaft rotor in hover, β_s / A_1. Comparison between the results of: a) A complete model. b) A model without wake distortion effects. c) A complete model with different aerodynamic matrices. d) Experimental results (Ref. 19).

It should also be noted that the experimental results exhibit certain phenomena in the range 7-12 Hz (see the sharp local increase in phase). This is not predicted by the numerical model and it may be the result of lead-lag effects, or again other effects that are missing.

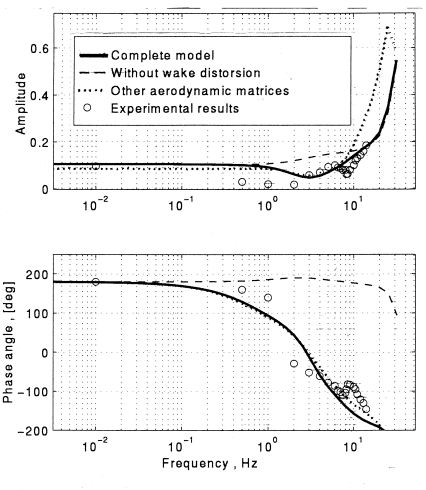

Fig. 3:The off-axis flapping response of a fixed shaft rotor in hover, β_c / A_1. Comparison between the results of: a) A complete model. b)A model without wake distortion effects. c) A complete model with different aerodynamic matrices. d) Experimental results (Ref. 19).

The off-axis flapping response results, β_c / A_1, are presented in Fig. 3. In this case wake distortion effects have a significant influence at frequencies in the range 1Hz - 10 Hz. The influence is especially large in the case of the phase angle, that in the presence of wake distortion exhibits sharp variations at frequencies higher than 1 Hz. The changes in the aerodynamic matrices have non-negligible influences only at relatively high frequencies, especially on the amplitude.

A comparison with the experimental results indicates that the complete model predicts a drop in amplitude at the frequency range 1-6 Hz that is also shown by the experimental results. Yet the experimental results exhibit a much larger drop, especially for 0.5-1 Hz. If wake distortion is neglected, the amplitude is gradually increased as the frequency is increased.

In the case of the phase angle, a model that does not include wake distortion does not exhibit the large change in phase angle except for very high frequencies (above 20 Hz). The complete model exhibits the correct change in the phase angle. Yet there are differences between the theoretical and experimental results, especially in the region 0.5-3 Hz, that probably are the results of the same reasons that resulted in differences in the on-axis response. Again, like in the case of the on-axis response, the experimental results exhibit certain phenomena in the range 7-12 Hz (local extremum in amplitude and phase) that are not predicted by the calculations.

5.2 The Frequency Response of a Hovering UH-60

The on-axis response in this case is the fuselage pitch response to longitudinal stick oscillations (q_f / lon) or fuselage roll response to lateral stick (p_f / lat).

In Fig. 4 the same three calculated results of Fig. 2, are compared with flight test results. It is shown that in the case of the on-axis response the influence of wake distortion effects is not large and appears at low frequencies. While wake distortion effects improve the agreement between the calculated and measured amplitudes, it somewhat worsens the agreement of the phase angles. The influence of the change in the aerodynamic matrices is relatively small, it presents a certain improvement in the amplitude of (p_f / lat) in the range 2-4 rad/sec. It should be noted that b in Eq. was chosen as 2. Choosing a value of b = 2.31 will give results that are very similar to those of the other aerodynamic matrices.

The off-axis response is shown in Fig. 5. It includes (q_f / lat) and (p_f / lon).

In the case of (q_f / lat) the agreement between the results of the complete model and the flight test results is fairly good throughout the entire range of frequencies. If the wake distortion effects are neglected, then very large differences appear in the amplitude over a wide range of frequencies. The known difference of 180º in phase, over a large range of frequencies is also evident. The influence of changing the aerodynamic matrices is relatively small.

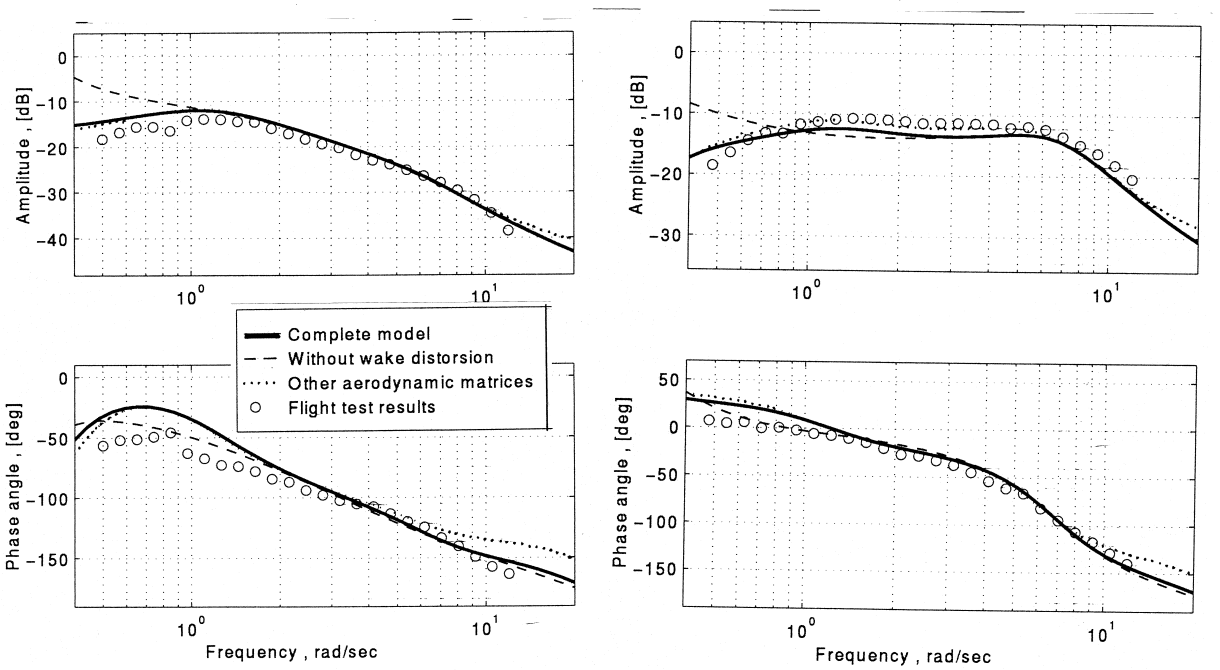

q_f / lon **p_f / lat**

Fig. 4: The on-axis response of a hovering UH-60. Comparison between the results of:
a) A complete model. b) A model without wake distortion effects.
c) A complete model with different aerodynamic matrices. d) Flight test results.

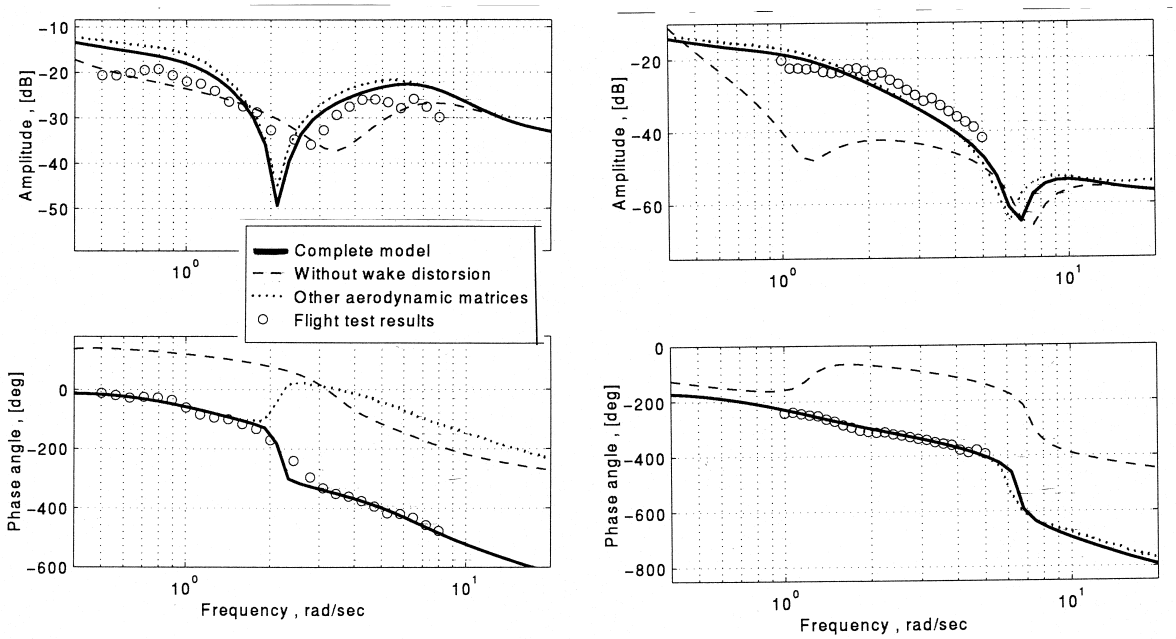

p_f / lon **q_f / lat**

Fig. 5: The off-axis response of a hovering UH-60. Comparison between the results of:
a) A complete model. b) A model without wake distortion effects.
c) A complete model with different aerodynamic matrices. d) Flight test results.

In the case of (p_f/lon) the agreement between the amplitude of the complete model and the flight test results is fair, with increasing differences at low frequencies. The minimum at medium frequencies, 1-2 Hz, appears in the both results. The influence on the amplitude of ignoring the wake distortion effects is smaller than in the case of (q_f/lat). Yet in the case of the phase angle, differences of 180º appear at low and medium frequencies (up to 2 Hz), if wake distortion effects are ignored. The influence of changing the aerodynamic matrices is relatively small and confined to higher frequencies. Please note that although in the case of (p_f/lon) the difference in phase seem to be large throughout all frequencies, for frequencies higher than 3 Hz the phase difference is roughly 360º, namely equivalent to zero. Investigations have shown that (p_f/lon) is very sensitive to small variations in the various parameters.

6. Conclusions

The derivation of a new approximate actuator disk model of a rotor during hover or axial flight has been presented. This model considers variations in the induced velocity over the disk as a result of variations in the loads along the blades, as well as wake distortion effects.

Two different approaches have been used to develop the model:

Both approaches describe the axial induced velocity through the disk by the three first terms in an infinite series: A uniform component together with sine and cosine components in azimuth that have a linear spanwise distribution. Five differential equations are obtained that describe these terms:

a) A single equation that describes the perturbation in the uniform component of the induced velocity due perturbations in the thrust coefficient and axial motion of the disk.
b) Two equations that describe the sine and cosine linear components of the perturbation, due to perturbations in the aerodynamic roll and pitch moment coefficients. These equations are analogous to the same equations in the dynamic-inflow model.
c) Two equations that describe variations in the linear sine and cosine components due to pitch and roll rates of the disk, namely, wake distortion effects.

All the models in the literature that added wake distortion effects to regular dynamic -inflow models combined the four equations, (b) and (c), to form two equations. It is shown here that this combination can be done only after special conditions are fulfilled. In general the two pairs of equations are separate.

In both approaches the velocity is calculated in a non inertial reference system - an axially moving, pitching and rolling reference system. In most of the simulation codes the induced velocity relative to an inertial system, that momentarily coincides with the disk system of coordinates, is used. Thus it is necessary to use the transformation between the non-inertial and inertial reference systems. A lack of doing this may result in increasing inaccuracies in the results.

The system of equations that are obtained by the two approaches are very similar, except for a coupling between two equations of (b) above, that exists in the results of the vortex approach and does not exit in the results of the momentum approach. Yet, numerical investigations showed that for most practical purposes this coupling is negligible and thus can be ignored. Therefore it can be concluded that both approaches lead to equivalent systems of equations.

Both approaches are based on certain approximations. One of the main approximations in the vortex model includes the neglect of higher order terms in the frequencies. This approximation may lead to increasing errors at high frequencies of the perturbations. Correction coefficients have been suggested to correct for certain approximations. These correction coefficients can be determined by applying a more refined theory. In the present analysis they have been determined such that a good agreement with experimental or flight test results is obtained.

The new model shows nice agreement with experimental and flight test results from the literature. It succeeds in improving significantly the results of the off-axis response, that otherwise exhibit large differences between theoretical and experimental results.

The form of the new model is very similar to that of the widely used dynamic-inflow model. Thus, the extension of existing codes that use the dynamic-inflow model, to also include the new model, is straightforward and can be done without facing any real difficulties.

Acknowledgement

The author would like to thank Mrs. B. Hirsch and Mrs. A. Goodman for typing the manuscript and Mrs. D. Rosen for the preparation of the figures.

References

1. Prouty, R.W., "The Case of the Cross-Coupling Mystery", Rotor & Wing, June, 1994, pp. 48-49.
2. Rosen, A. and Isser, A., "A New Model of Rotor Dynamics During Pitch and Roll of a Hovering Helicopter", J. of the American Helicopter Society, Vol. 40, No. 3, 1995, pp. 17-28. (Also Proceedings of the 50th Annual Forum of the American Helicopter Society, Washington DC, May 11-13, 1994, pp. 409-426.)
3. Isser, A. and Rosen, A., "The Pitch Damping of a Hovering Rigid Rotor", J. of the American Heli- copter Society, Vol. 42, No. 1, 1997, pp. 96-99.

4. Pitt, D.M. and Peters, D.A., "Theoretical Prediction of Dynamic-Inflow Derivatives", Vertica, Vol. 5, 1981, pp. 21-34.
5. Peters, D.A. and He, C.J., "A Closed-Form Aerodynamic Theory for Lifting Rotors in Hover and Forward Flight", 43rd Annual Forum of the American Helicopter Society, Saint Louis, Missouri, May 18-20, 1987, pp. 839-865.
6. Keller, J.D., "An Investigation of Helicopter Dynamic Coupling Using an Analytical Model", J. of the American Helicopter Society, Vol. 41, No. 4, 1996, pp. 322-330. (Also Proceedings of the 21st European Rotorcraft Forum, St. Petersburg, Russia, August 1995.)
7. Arnold, U.T.P., Keller, J.D., Curtiss, H.C. and Reichert, G., "The Effect of Inflow Models on the Predicted Response of Helicopters", J. of the American Helicopter Society, Vol. 43, No. 1, 1998, pp. 25-36. (Also Proceedings of the 21st European Rotorcraft Forum, St. Petersburg, Russia, August 1995.)
8. Krothapalli, K.R., Prasad, J.V.R. and Peters, D.A., "Development of a Comprehensive Wake Theory for Lifting Rotors", AIAA Atmospheric Flight Mechanics Conference, San Diego, CA, July 1996, AIAA-96-3390, pp. 767-772.
9. Barocela, E., Peters, D.A., Krothapalli, KR., and Prasad, J.V.R., "The Effect of Wake Distortion on Rotor Inflow Gradients and Off-Axis Coupling", AIAA Atmospheric Flight Mechanics Conference, New Orleans, LA, August 1997, AIAA-97-3579, pp. 272-282.
10. Krothapalli, K.R., Prasad, J.V.R. and Peters, D.A., "A Generalized Dynamic Wake Model with Wake Distortion", Proceedings of the 54th Annual Forum and Technology Display of the American Helicopter Society, Washington D.C., May 1998, pp. 527-536.
11. Krothapalli, K.R., Prasad, J.V.R. and Peters, D.A., "Helicopter Rotor Dynamic Inflow Modeling for Maneuvering Flight", Proceedings of the 55th Annual Forum of the American Helicopter Society, Montreal, Canada, April 1999, pp. 498-510.
12. Bagai, A., Leishman, J.G. and Park, J., "Aerodynamic Analysis of a Helicopter in Steady Maneuvering Flight Using a Free-Vortex Rotor Wake Model", J. of the American Helicopter Society, Vol. 44, No. 2, 1999, pp. 109-120 (a revised version of a paper presented at the AHS Technical Specialists' Meeting on Rotorcraft Acoustics and Aerodynamics, Williamsburg, VA, October 1997).
13. Park, J.S. and Leishman, J.G., "Investigation of Unsteady Aerodynamics on Rotor Wake Effects in Maneuvering Flight", Proceedings of the 55th Annual Forum of the American Helicopter Society, Montreal, Canada, May 1999, pp. 467-480.
14. Basset, P.-M. and Tchen-Fo, F., "Study of the Rotor Wake Distortion Effects on the Helicopter Pitch-Roll Cross-Couplings", 24th European Rotorcraft Forum, Marseilles, France, September 1998, FMO6.1-FMO6.13.
15. Keller, J.D. and Curtiss, H.C., "A Critical Examination of the Methods to Improve the Off-Axis Response Prediction of Helicopters", Proceedings of the 54th Annual Forum of the American Helicopter Society, Washington D.C., May 1998, pp. 1134-1147.
16. Hammers, M. and von Grunhagen, W., "Nonlinear Helicopter Model Validation Applied to Realtime Simulations", 53rd Annual Forum of the American Helicopter Society, Virginia Beach, Virginia, April 29 - May 1, 1997, pp. 958-972.
17. He, Chengjian, He, C.S. and Chen, Weibin, "Rotorcraft Simulation Model Enhancement to Support Design, Testing and Operational Analysis", Proceedings of the 55th Annual Forum of the American Helicopter Society, Montreal, Canada, May 1999, pp. 2122-2139.
18. Theodore, C.R. and Celi, R., "Flight Dynamic Simulation with Refined Aerodynamics and Flexible Blade Modeling", Proceedings of the 56th Annual Forum of the American Helicopter Society, Virginia Beach, Virginia, May 2000, pp. 857-872.
19. Tchen-Fo, F., Eglin, P., Gimoret, B., Desoper, A., Hellard, S., von Gruenhagen, W. and Roth, G., "Comparison Between Experimental and Predicted Isolated Helicopter Rotor Transfer Functions for Unsteady Inputs on the Controls", Proceedings of the 56th Annual Forum of the American Helicopter Society, Virginia Beach, Virginia, May 2000, pp. 911-927.
20. Hamers, M. and Basset, P.M., "Application of the Finite State Unsteady Wake Model in Helicopter Flight Dynamic Simulation", Proceedings of the 26th European Rotorcraft Forum, The Hague, The Netherlands, September 2000, pp. 27.1-27.16.
21. Isser, A. and Rosen, A., "A Model of the Unsteady Aerodynamics of a Hovering Helicopter Rotor that Includes Variations of the Wake Geometry", J. of the American Helicopter Society, Vol. 40, No. 3, 1995, pp. 6-16. (Also Proc. of the 34th Israel Annual Conference on Aerospace Sciences, February 1994, pp. 90-105.)
22. Curtiss, H.C., "Aerodynamic Models and the Off- Axis Response", Proceedings of the 55th Annual Forum of the American Helicopter Society, Montreal, Canada, May 1999, pp. 2037-2040.
23. Moon, P. and Spencer, D.E., *Field Theory Handbook: Including Coordinate Systems Differential Equations and Their Solutions*, Springer, Berlin, 2nd Ed. 1971, 236 p.
24. Glauert, H., "On the Contraction of the Slipstream of an Air-Screw", Aeronautical Research Council R&M No. 1067, 1926.
25. Finlayson, B.A., *The Method of Weighted Residuals and Variational Principles*, Academic Press, N.Y. 1972, 412 p.
26. Miller, R.H., "Rotor Blade Harmonic Loading", AIAA J., Vol. 2, No. 7, 1964, pp. 1254-1269.
27. Baskin, V.E., Vil'dgrube, L.S., Vozhdayev, Ye.S. and Maykapur, G.I., "Theory of the Lifting Airscrew", NASA TT F-823, 1976 (English translation of the 1973 Russian publication).
28. Stepniewski, W.Z. and Keys, C.N., "*Rotary-Wing Aerodynamics - Vol. 1, Basic Theories of Rotor Aerodynamics*", Dover Publications Inc. New York, 1984.
29. Allongue, M. and Drevet, J.P., "New Rotor Test Rig in the Large Modane Wind Tunnel", 15th European Rotorcraft Forum, Amsterdam, September 12-15, 1989, Paper No. 98.
30. Crozier, P., Eglin, P and Desopper, A., "Determination of Isolated Rotor Transfer Functions in the ONERA S1.MA Wind Tunnel", 24th European Rotorcraft Forum, Marseilles, France, 15-17 September 1998, Paper TE04.
31. Rosen, A., "Approximate Actuator Disk Model of a Rotor During Hover or Axial Flow", Faculty of Aerospace Engineering, Technion, TAE Report 873, June 2001, 93 p.